JOURNAL OF Materials CHEMISTRY

Synthesis of rod-, twinrod-, and tetrapod-shaped CdS nanocrystals using a highly oriented solvothermal recrystallization technique

Meng Chen, Yi Xie,* Jun Lu, Yujie Xiong, Shuyuan Zhang, Yitai Qian and Xianming Liu

Structure Research Lab and Department of Chemistry, University of Science & Technology of China, Hefei, Anhui 230023, P. R. China. Tel: 86-551-3603987; Fax: 86-551-3603987; E-mail: yxie@ustc.edu.cn

Received 27th June 2001, Accepted 23rd November 2001
First published as an Advance Article on the web 23rd January 2002

Rod-, twinrod- and tetrapod-shaped CdS nanocrystals have been successfully prepared from the starting spherical CdS nanocrystals *via* a highly oriented solvothermal recrystallization technique. X-Ray powder diffraction, X-ray photoelectron spectroscopy, transmission electron microscopy and high-resolution transmission electron microscopy have been used to characterize the crystal structure and growth direction of the obtained sample. The present technique may open a new doorway to one-dimensional nanosized semiconductors from the same kind of materials with irregular shape or larger size.

Introduction

During the past decade, the trend in nanoparticle synthetic research has been expanded beyond studies of quantum dots to include morphological control of inorganic nanoparticles.[1–9] These research efforts have been driven by the exciting possibility of creating tailor-designed nanostructural materials with unique electrical and optical properties[10,11] For example, a single-walled carbon nanotube (SWNT) can be metallic, semiconducting, or semimetallic, depending on its chirality.[12] The tunability of the lattice orientation in the silicon nanowires could lead to different optical properties.[13] However, the shape control and size tunability of nanocrystals remains difficult and very laborious work to many researchers.

A variety of nanofabrication techniques and crystal growth methods have been used to achieve shape control, especially to fabricate 1D semiconductor materials. Of these techniques to 1D nanocrystals in either a physical or chemical basis, the more general, yet relatively simple, pathway still begins with choosing ideal templates, and then initiating the reaction and the crystal nucleation and growth. Nanotubes,[14] porous anodic aluminium oxide (AAO)[15–18] and nuclear track-etched polycarbonate membranes[19–21] have been applied as templates to prepare semiconductor nanowires. Another kind of template, such as regular or inverse micelles,[22–24] liquid crystal,[25] polymer[26] and some biological assemblies,[27] have also been employed as 'soft templates' to control the morphology of nanocrystals, mainly *via* the chemical interaction between the reactants and templates.

Over the past several years, one-dimensional semiconductor nanomaterials have been obtained without a template but in a specific organic solvent. Korgel and coworkers[13] have successfully directed uniform, defect-free silicon (Si) nanowire growth in supercritical hexane with a silicon precursor, diphenylsilane, at a temperature of 500 °C and 270 bar. Buhro's group[28] have reported the crystallization of the Group III–V compounds, in unusual polycrystalline fiber and whisker morphologies with small crystal dimensions, using simple organometallic reactions conducted at low temperatures ($\leqslant$203 K) in hydrocarbon solvents. Meanwhile, The solution–liquid–solid growth mechanism in which a solid rod grows out of a flux droplet has been proposed to explain the formation of 1D nanostructures in liquid media.

Owing to the great chemical flexibility and synthetic tunability in the solution-phase syntheses,[13] the highly controlled solution-phase self-assembly method has been successfully extended to vary the shapes of the resulting Group II–VI semiconductor particles. The shape of colloidal CdSe nanocrystals can be effectively manipulated by the decomposition of organometallic precursors in a hot (*ca.* 300 °C) mixture of trioctylphosphine oxide and hexylphosphonic acid (HPA),[7,9] and with the similar synthetic process, high-quality, shape-controlled CdTe nanorods could also be obtained.[29] The controlled formation of CdSe nanocrystals with diverse morphologies can be attributed so that the HPA could accentuate the differences in the growth rates among the various faces of the nanocrystals. Our research group, using many kinds of cadmium and sulfur sources, obtained CdE (E = S, Se and Te) nanorods in ethylenediamine by a solvothermal process.[2,30–32] The formation process of CdS nanorods has been discussed in detail,[32] and the CdS nanorods were found to have been formed through an accordion-like folding process that was caused by the dissociation of the ethylenediamine molecules adsorbed on the surface of CdS. In our opinion, ethylenediamine plays the same role in the anisotropic growth of CdE nanocrystals as that of HPA in the growth of CdSe nanorods.

By the solvothermal process, however, CdS nanocrystals with either a spherical or rod-like shape have been obtained. No other shapes of CdS nanoparticles have been observed. The growth direction of CdS nanorods was deduced only from the XRD patterns of the samples. In addition, the CdE (E = S, Se, Te) nanorods reported previously were all obtained through various chemical reactions from raw materials. For example, CdS nanorods could be prepared by the reaction of Cd powder[30] or CdC_2O_4[2] with elemental S, or $Cd(NO_3)_2$ with NH_2CSNH_2[32] in ethylenediamine. Herein, we demonstrate the variation of the shape of CdS nanoparticles, for the first time, using a highly oriented solvothermal recrystallization technique. HRTEM was employed to characterize the crystal structure and growth direction of rod-shaped nanocrystals. High quality CdS nanocrystals with different morphologies were prepared mainly from CdS particles, which avoid not only the introduction of the heterogeneous ions such as NO_3^- and $C_2O_4^{2-}$ besides Cd^{2+} and S^{2-} during the reaction process, but also the excess of Cd^{2+} or S^{2-}. Moreover, spherical CdS nanocrystals were used as the starting materials, and the morphologies of the resulting CdS nanocrystals can be easily controlled by suitable variation of the recrystallization temperature, the ratio of Cd to S atoms, the solvent and the

 DOI: 10.1039/b105652m

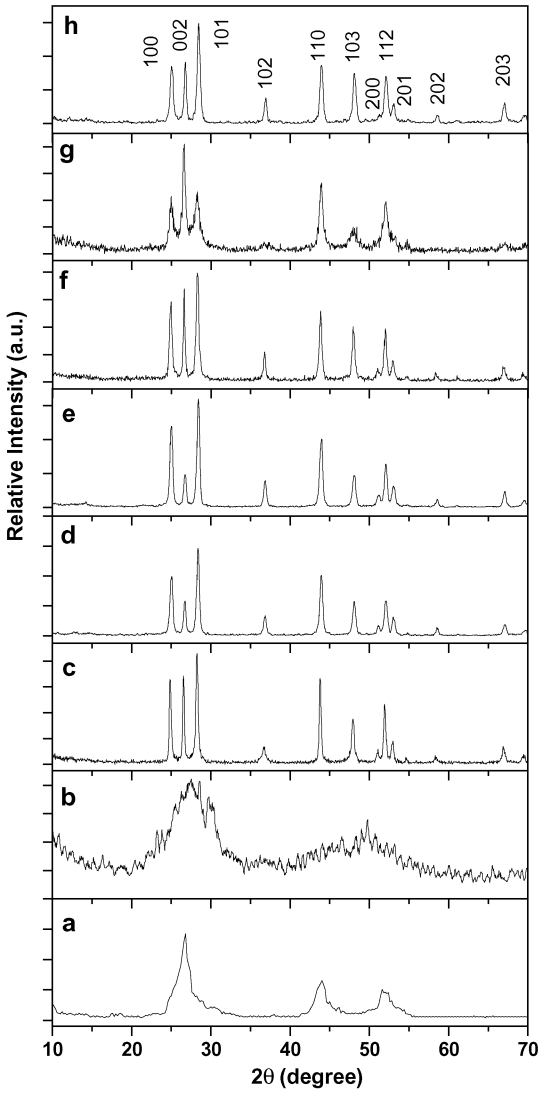

Fig. 1 XRD patterns of (a) the starting CdS nanocrystals obtained by γ-irradiating the solution containing Cd^{2+} and sulfur, such as $Na_2S_2O_3$ or CS_2; (b) the starting amorphous CdS nanoparticles prepared from the reaction of $CdCl_2$ with Na_2S in the solvent mixture at room temperature; (c–e) the resulting CdS nanorods prepared in ethylenediamine at 140 °C by solvothermal recrystallized treatment from 0.1, 0.2 and 0.5 g of the starting CdS nanoparticles, respectively, air-cooling used; (f) the short CdS nanorods prepared in aqueous ammonia from 0.2 g of the starting CdS nanoparticles, and air-cooling used; (g) the twinrod CdS nanocrystals prepared from 0.2 g of the starting CdS nanoparticles in ethylenediamine at 180 °C, and water-cooling used; (h) the tetrapod CdS nanocrystals prepared by keeping 0.3 g of CdS nanocrystals in ethylenediamine at 180 °C for 5 h and then cooling the resulting solution to room temperature at the rate of 10 °C h^{-1}.

initial CdS content. Actually, CdS nanocrystals can be easily obtained by many methods, and the results imply that the route to CdS nanocrystals may not be of much importance, if CdS nanoparticles can be synthesized by other means. Thus, the present study provides a novel route to high quality semiconductor nanocrystals with different morphologies from the same kind of materials with irregular or larger sizes, and the scheme can be readily scaled up for industrial production.

Experimental

Synthesis

The starting materials were spherical CdS nanocrystals and non-crystalline CdS nanoparticles. Spherical CdS nanocrystallines with diameters of less than 6 nm could be obtained by the γ-irradiation technique described elsewhere.[33] In brief, the procedure involved irradiating the solution containing Cd^{2+} and sulfur such as $Na_2S_2O_3$ or CS_2. Amorphous CdS nanoparticles could easily be prepared by the reaction of $CdCl_2$ with Na_2S in the solvent mixture at room temperature. In a typical solvothermal recrystallization process to CdS crystals, an appropriate amount of CdS particles was put into an autoclave of 20 ml and then the autoclave was filled with a suitable solvent up to 85% of the total volume. The autoclave was maintained at a fixed temperature for 5 h and then left to air or water cool to room temperature (< 20 °C). The precipitate was filtered off and washed sequentially with distilled water and absolute ethanol. After being dried in a vacuum at 50 °C for 4 h, a yellow final product was obtained for further analysis.

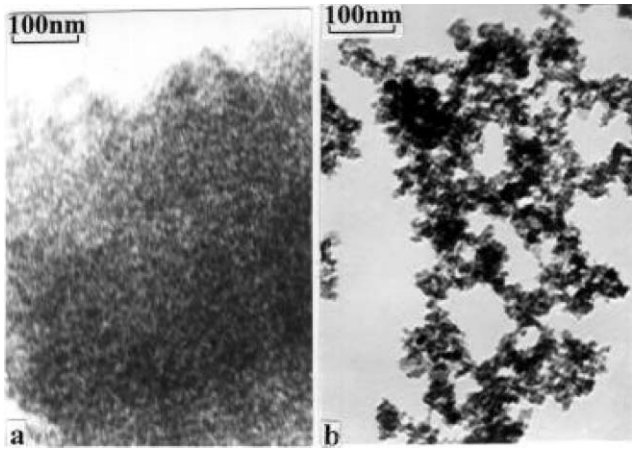

Fig. 2 TEM images of the starting CdS nanoparticles obtained (a) by γ-irradiation, (b) at room temperature.

Characterization

X-Ray powder diffraction (XRD) patterns were recorded using a Japan Rigaku D/max γ_A-ray diffractometer with Ni-filtered Cu-Kα radiation ($\lambda = 1.54178$ Å). Nanocrystals were placed on quartz plates for measurement. X-Ray photoelectron spectroscopy (XPS) spectra were obtained on a VGESCALAB MKII X-ray photoelectron spectrometer, using Mg-Kα radiation as the excitation source. The morphologies and particle sizes of samples were determined by transmission electron microscopy (TEM). The images were taken with a Hitachi H-800 transmission electron microscope, using an accelerating voltage of 200 kV. Average length and size distributions were determined on the order of 200 nanocrystals per sample for statistical purposes. High-resolution transmission electron microscopy (HRTEM) was carried out on a JEOL-2010 transmission electron microscope.

Results and discussion

The starting CdS nanoparticles

Based on the previous study[33] and JCPDS data (No. 10-454[#] and 41-1049[#]), the X-ray powder diffraction (XRD) pattern of the starting spherical CdS particles (Fig. 1a) obtained by γ-irradiation could be indexed as a mixture of cubic sphalerite CdS with hexagonal wurtzite CdS as a minor component. The XRD pattern for amorphous CdS particles (Fig. 1b), prepared from the reaction of $CdCl_2$ with Na_2S in the solvent mixture at room temperature, showed only the diffuse peaks corresponding to the scattering of the non-crystalline CdS particles. TEM images of the starting nanocrystalline and amorphous CdS (Fig. 2a,b) illustrate these solid semiconductor clusters with a near spherical shape.

Rod-shaped nanocrystals

Rod-shaped CdS nanocrystals with uniform diameters of 40 nm and lengths up to 8 μm can be readily obtained in ethylenediamine from either spherical crystalline or non-crystalline CdS particles. The recrystallization temperature was 140 °C and the resulting solution was air cooled to room temperature. The average length of the synthesized nanorods mainly depended upon the amount of the starting CdS nanoparticles. Fig. 3a–c shows the TEM photographs and size distribution of the rod-shaped CdS nanocrystals produced at different initial CdS contents. When the amount of spherical CdS nanocrystals was increased from 0.1 to 0.2 and 0.5 g in 18 ml of ethylenediamine, the average length of the obtained CdS nanorods changed from 0.4 to 2.9 and 1.4 μm, respectively. All the obtained higher quality CdS nanorods have uniform diameters and larger aspect ratios up to 200 compared with those reported.[2,30,32] The XRD patterns of the resulting CdS nanorods (Fig. 1c–e) exhibited reflections for hexagonal CdS with lattice constants consistent with the values of JCPDS 41-1049. Moreover, there were a few stronger peaks of (100) and (110), together with a weaker peak of (002) (Fig. 1d,e) than was expected from the powder diffraction of bulk CdS, which suggested that the [001] direction was aligned along the nanorod axis and that CdS nanocrystals mainly lie on the surface of silicon for XRD characterization.[34] It is interesting to observe that the reported CdS nanorods with the strongest intensity of the (002) diffraction peak have the same preferential orientation along the *c* axis.[30,32] This indicated that the crystal growth direction of nanorods was mostly perpendicular to the substrate in the XRD measurements. The difference in the manner in which CdS nanorods lay down or stand on the surface of the silicon resulted from the fact that those as-obtained nanorods had different aspect ratios. Since all the nanorods have nearly uniform diameters, the longer the nanorods, the larger the aspect ratio, and the more nanorods lie on the surface of silicon. Roughly speaking, most of the nanorods were longer than 1 μm in the present study whereas those nanorods were generally shorter than 1 μm in the previous reports.

The longest and highest quality CdS nanorods were obtained in 18 ml of ethylenediamine at 150 °C using 0.2 g of spherical CdS nanocrystals with diameters of less than 6 nm as the starting materials, then air cooled to room temperature. Typical TEM images of the sample (Fig. 3d) show the straight CdS nanorods with diameters of *ca.* 40 nm and lengths of up to 8 μm. The lattice fringes of CdS in the wurtzite structure, as well as some stacking faults, could be clearly observed (Fig. 1e), which showed the fine structure of the rod-like CdS particles.

The solvent used in this process also affected the morphology of the product. Only spherical or irregular CdS nanocrystals could be obtained by replacing ethylenediamine with ethanol or benzene. Interestingly, shorter and thicker CdS nanorods, with diameters ranging from 30 to 60 nm and lengths of *ca.* 50–200 nm, could be obtained in aqueous ammonia (Figs. 1f and 4a). The weaker coordinating solvent, compared with ethylenediamine, still plays a crucial role in controlling the orientation growth.

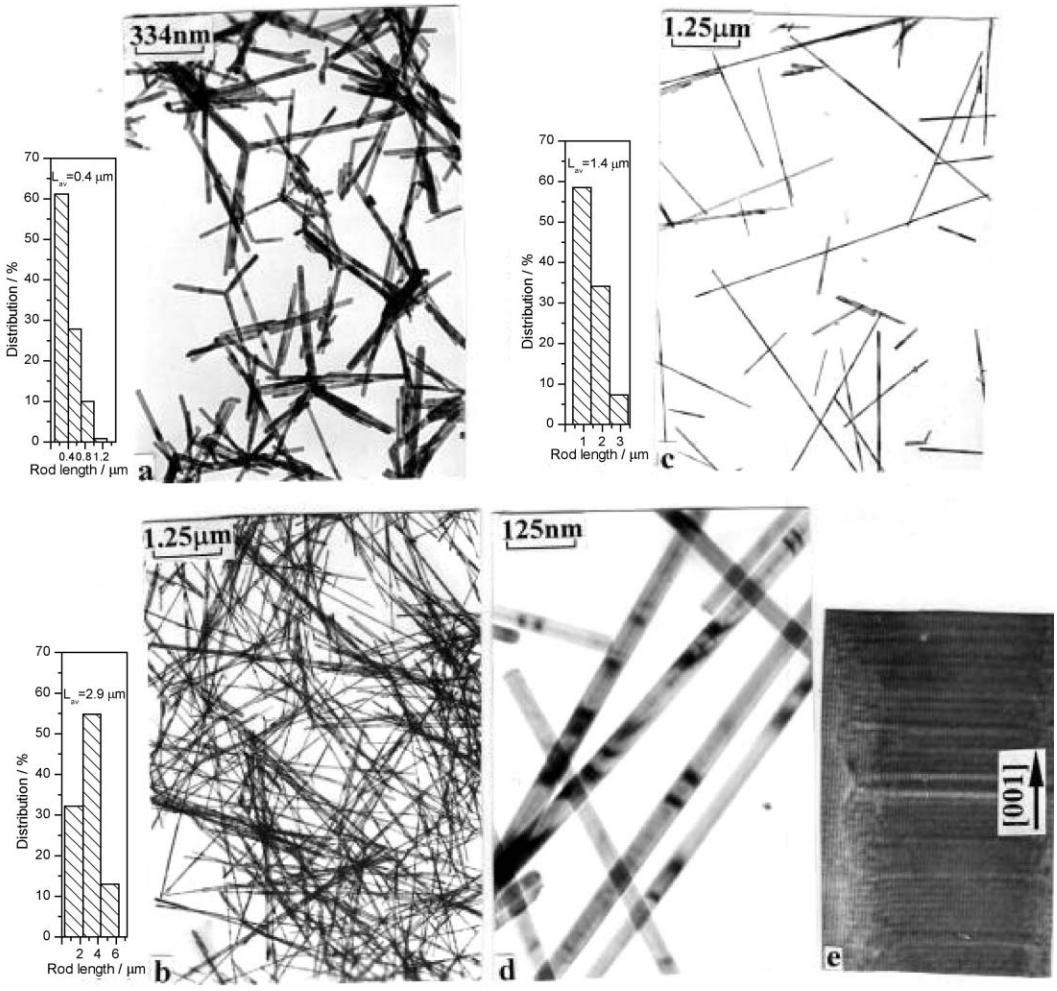

Fig. 3 TEM images and histograms of the size distributions of the resulting CdS nanorods prepared in ethylenediamine at 140 °C by solvothermal recrystallization treatment from 0.1 (a), 0.2 (b) and 0.5 g (c) of the starting CdS nanoparticles, respectively, air-cooling used. (d) TEM image and HRTEM image of high quality CdS nanorods.

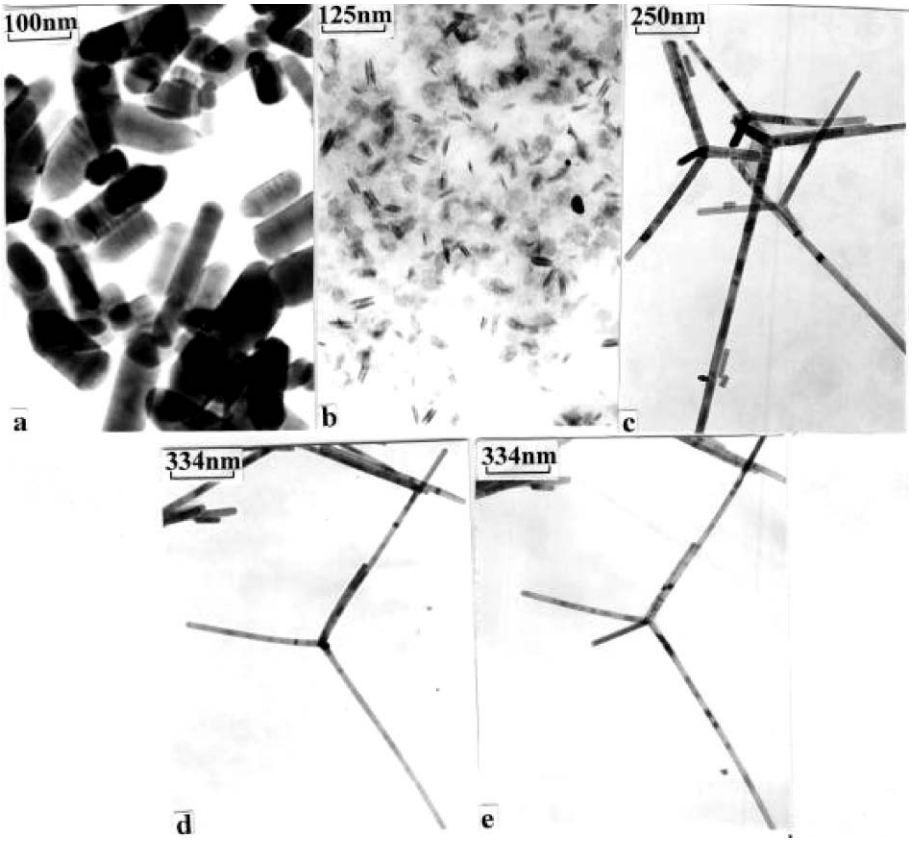

Fig. 4 TEM images of (a) the short and thick CdS nanorods, (b) the twinrod CdS nanocrystals, (c) the tetrapod CdS nanocrystals, and (d–e) a typical tetrapod CdS nanocrystal showing three arms and four arms by suitable rotation.

Twinrod nanocrystals

Another nanocrystal shape which could be obtained in ethylenediamine is the twinrod CdS nanocrystals, as seen in Fig. 4b. The starting solution consisted of spherical CdS nanocrystals and sulfur powder (1 : 6), the recrystallization temperature was 180 °C, and water cooling was used to lower the temperature of the resulting solution from 180 °C to room temperature within 2 h. The XRD pattern shown in Fig. 1g demonstrated that the products were not very well crystallized compared with those of other samples show in Fig. 1c–e, which may be attributed to the sudden temperature drop. The XPS spectra confirmed the formation of CdS nanocrystals with the molar ratios of CdS of 1 : 1.1. Typical TEM images revealed that twinrod-shaped nanocrystals were composed of two aligned nanorods with similar diameters (<6 nm), spacing (*ca.* 6–15 nm) and length (*ca.* 10–50 nm).

Although the detailed formation mechanism of the twinrod nanocrystals is not clear, the sudden temperature drop and excess of sulfur powder may be responsible for their formation, which could result in a short burst of homogeneous nucleation, and then prevent the further nucleation. Further evidence about the influence of the sudden temperature drop on CdS shape comes from the fact that nearly spherical rather than rod-shaped CdS nanocrystals are mainly contained in the sample prepared without the addition of sulfur powder and keeping other conditions constant.

Tetrapod-shaped nanocrystals

Large numbers of tetrapod CdS nanocrystals, in which four arms grown out of a tetrahedral center as shown in Fig. 4c, were observed in the sample prepared by keeping 0.3 g of CdS nanocrystals in ethylenediamine at 180 °C for 5 h and then cooling the resulting solution to room temperature at a rate of 10 °C h^{-1}. In fact, there were a few tetrapod CdS nanocrystals in the previous sample (Fig. 2a). Lattice fringes persisting throughout the entire crystals are shown in Fig. 5b, suggesting crystallinity in both the center and the arms. Some tripod-shaped nanocrystals could be observed in TEM images because the long axis of the fourth rod was parallel to the direction of the electron beam of the instrument. Four arms can be clearly observed if the sample is rotated to certain angles, which was confirmed by Fig. 4d,e.

The present study shows the interesting phase and shape

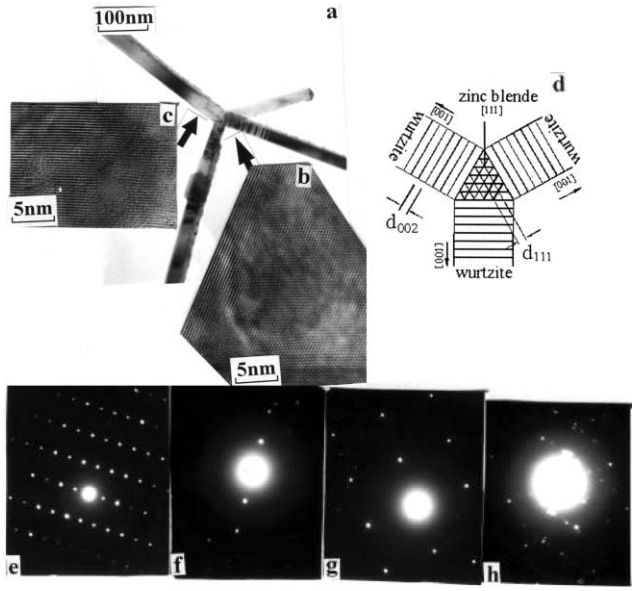

Fig. 5 Typical tetrapod-shaped CdS nanocrystals: (a) TEM image, (b) HRTEM image of the starting nuclei, (c) HRTEM image of one arm, (d) two-dimensional representation showing the structure image and growth direction, where three are shown with the fourth coming out of the page towards the reader, (e–h) selected-area ED pattern of the three arms and the center (shown in c).

transformation of CdS nanocrystals, from sphalerite to wurtzite, from spherical to rod shape, as well as shape control in the solvothermal recrystallization process. It is well known that CdS generally shows dimorphism of sphalerite and wurtzite type at relatively low temperatures and only wurtzite type at higher temperatures. The only structure difference between hexagonal and cubic CdS is in the close-packing: the former has an ABAB structure, whereas the latter is ABCABC packed.[35] Few reports[36,37] are available on cubic to pure hexagonal phase transformation in CdS, which were all performed at more than 300 °C. For example, Zelaya-Angel and Lozada-Morales observed a transition from cubic to hexagonal structure in thin CdS films upon heating in Ar.[37] In the present study, a similar transformation was also observed at no more than 180 °C. Moreover, the morphologies of CdS nanocrystals varied from spherical particles to rod-like crystals. In our opinion, the dissolution of CdS nanoparticles in ethylenediamine and the orientation correction of solvent molecules may well be responsible for the observed phase and shape transition of CdS nanocrystals. Briefly, at relatively elevated temperatures and under certain pressures, CdS particles may be gradually dissolved in ethylenediamine and form the complex of ethylenediamine with Cd ions, followed by the nucleation and growth of CdS rods with any decrease in temperature. There are many reports about the growth mechanism of CdS nanorods in ethylenediamine.[2,30–32]

Variation of the initial CdS content in ethylenediamine plays an important role in determining the length of the rod-shaped nanocrystal. This is clearly seen in the experiments where the CdS content is varied (Fig. 3a–c). In the CdS nanocrystal growth, there is a reversible pathway (dissolution and crystallization) between a fluid solution phase and the solid phase, which allows atoms, ions and molecules to adopt correction positions in the developing crystal lattices. Thus, as the favorable CdS content is chosen, small rods dissolve and larger ones grow longer, although the distribution of the CdS sizes is slightly broadened. If at higher CdS content, decreasing the temperature induces the germination of a high number of nuclei in solution, small particles grow faster than the longer ones, leading to the shorter nanorods. Similar results have also been found by Peng *et al.*[9]

With an increase of the recrystallization temperature, the shape and structure of CdS nanorods changes from rod-shaped nanocrystals to tetrapod-shaped nanocrystals as shown in Fig. 4c. This still can be understood as arising from the temperature dependence of the solubility of CdS nanocrystals in ethylenediamine. At lower temperatures (140 °C), only part of the CdS nanoparticles can be dissolved in ethylenediamine and the growth of rod-shaped particles mainly occurs on the bottom of the autoclave, and thus the rod-shaped nanocrystals are formed (Fig. 3a–c). At a recrystallization temperature of less than 120 °C, in particular, spherical CdS nanocrystals make up a larger proportion of the observed sample, which further supports the conclusion. At relatively higher temperatures (180 °C), all CdS nanocrystals can be dissolved and the growth of CdS nanorods homogeneously occurs in ethylenediamine, and enough energy ensures the growth of tetrapod-shaped nanocrystals in the preferential growth of crystal faces of CdS (Fig. 4c). Actually, Ostwald ripening occurs during this process, and that is to say, small nanocrystals dissolve at the expense of grown larger ones.

To the best of our knowledge, no report about this interesting result on the formation of tetrapod-shaped CdS nanocrystals has been given up to now. We consider that the formation mechanism of tetrapod CdS nanorods is similar to that of tetrapod-shaped CdSe nanocrystals,[7] which was reported very recently by Alivisatos *et al.* Those CdSe tetrapods were prepared by using thermal decomposition of organometallic precursors in a hot (300 °C) mixture of trioctylphosphine oxide and hexylphosphonic acid. In the crystal growth of CdS, the preferential growth face is (111) for the sphalerite structure and the (001) face for a wurtzite structure. The starting nucleus for tetrapod nanocrystals is the tetrahedral sphalerite (zinc blende) structure, and wurtzite arms grow out of each of the four (111) equivalent faces, then evolve into tetrapod-shaped CdS along the *c* axis. To visualize better the structure and growth direction of the tetrapod nanocrystals, a simulation of the lattice fringes has been constructed, as shown in Fig. 5d. A HRTEM image recorded on the nuclei and common boundary of tetrapod nanorods exhibits good crystallinity and well-resolved lattice fringes. This provides further insight into their structure, showing that it conforms perfectly to the simulated pattern, thus supporting the proposed growth mechanism. Fig. 5c shows clearly the structure image of one arm with an interplanar spacing of *ca.* 3.35 Å, corresponding to the (002) plane of wurtzite CdS. Selected-area electron diffraction patterns of three arms and the core (Fig. 5e–h) confirms that it is a single crystal, and all patterns are indexed to the reflection of hexagonal CdS crystals along the *c* axis. The discrepancy in the ED patterns of the three arms is due to the fact that the arms are non-uniplanar. Fig. 5b demonstrates many cross fringes of the center of the tetrapod nanocrystal, which are very different from those of other arms. The spaces of *ca.* 3.35 Å correspond to the distances between two (111) planes of the zinc blende CdS crystals. The ED pattern of the core revealed that the CdS nanocrystals are in the wurtzite structure owing to the extremely small portion of zinc blende CdS.

Especially herein, the starting materials are mainly zinc blende CdS nanocrystals, which play the part of seed crystals, and are epitaxially grown to wurtzite CdS nanorods by the solvothermal treatment at 180 °C. Actually, epitaxial growth of wurtzite layers out of a zinc blende core has been reported.[38] Therefore, the tetrapod-shaped CdS nanocrystals make up more than 80% of the total CdS nanorods observed in the TEM image.

Conclusions

The present study describes an easily controlled and reproducible solvothermal recrystallization technique, which can be used to prepare high quality and oriented CdS nanocrystals with rod, twinrod or tetrapod shapes. The formation mechanism of CdS nanocrystals with different morphologies has been discussed in detail. It has been found that the crystallization temperature, the initial CdS content and cooling method play crucial roles in the formation of one-dimensional CdS nanocrystals. We have also successfully extended this synthetic method to the production of one-dimensional PbS crystals; however, up to now synthetic conditions have not yet been optimized to produce a sample quality comparable to that of the CdS nanoparticles.

Acknowledgements

Financial support from the National Natural Science Foundation of China and Chinese Ministry of Education are gratefully acknowledged.

References

1 J. A. Haber, P. C. Gibbons and W. E. Buhro, *J. Am. Chem. Soc.*, 1997, **119**, 5455.
2 S. H. Yu, Y. S. Wu, J. Yang, Z. H. Han, Y. Xie, Y. T. Qian and X. M. Liu, *Chem. Mater.*, 1998, **10**, 2309.
3 S. H. Yu, J. Yang, Z. H. Han, Y. Zhou, R. Y. Yang, Y. T. Qian and Y. H. Zhang, *J. Mater. Chem.*, 1999, **9**, 1283.
4 L. N. Wang and M. Muhammed, *J. Mater. Chem.*, 1999, **9**, 2871.
5 P. V. Braun, P. Osenar, V. Tohver, S. B. Kennedy and S. I. Stupp, *J. Am. Chem. Soc.*, 1999, **121**, 7302.

6 D. C. Nesting, J. Kouvetakis and D. J. Smith, *Appl. Phys. Lett.*, 1999, **74**, 958.
7 L. Manna, E. C. Scher and A. P. Alivisatos, *J. Am. Chem. Soc.*, 2000, **122**, 12 700.
8 S. Q. Feng, D. P. Yu, H. Z. Zhang, Z. G. Bai and Y. Ding, *J. Cryst. Growth*, 2000, **209**, 513.
9 X. G. Peng, L. Manna, W. D. Yang, J. Wickham, E. Scher, A. Kadavanich and A. P. Alivisatos, *Nature*, 2000, **404**, 59.
10 A. P. Alivisatos, *Science*, 1996, **271**, 933.
11 C. M. Lieber, *Solid State Commun.*, 1998, **107**, 607.
12 M. S. Dresselhaus, G. Dresselhaus and P. C. Eklund, *Science Of Fullerenes and Carbon Nanotubes*, Academic Press, San Diego, CA, 1996.
13 J. D. Holmes, K. P. Johnston, R. C. Doty and B. A. Korgel, *Science*, 2000, **287**, 1471.
14 W. Q. Han, S. S. Fan, Q. Q. Li and Y. D. Hu, *Science*, 1997, **277**, 1287.
15 D. Routkevitch, T. Bigioni, M. Moskovits and J. M. Xu, *J. Phys. Chem.*, 1996, **100**, 14 037.
16 J. S. Suh and J. S. Lee, *Chem. Phys. Lett.*, 1997, **281**, 384.
17 D. S. Xu, X. S. Shi, G. L. Guo, L. L. Gui and Y. Q. Tang, *J. Phys. Chem. B*, 2000, **104**, 5061.
18 D. S. Xu, Y. J. Xu, D. P. Chen, G. L. Guo, L. L. Gui and Y. Q. Tang, *Adv. Mater.*, 2000, **12**, 520.
19 C. R. Martin, *Science*, 1994, **266**, 1961.
20 C. R. Martin, *Chem. Mater.*, 1996, **8**, 1739.
21 V. M. Cepak and C. R. Martin, *J. Phys. Chem. B*, 1998, **102**, 9985.
22 Y. Y. Yu, S. S. Chang, C. L. Lee and C. R. C. Wang, *J. Phys. Chem. B*, 1997, **101**, 6661.
23 L. M. Qi, J. M. Ma, H. M. Cheng and Z. G. Zhao, *J. Phys. Chem. B*, 1997, **101**, 3460.
24 B. Nikoobakht, Z. L. Wang and M. A. El Sayed, *J. Phys. Chem. B*, 2000, **104**, 8635.
25 Y. Li, J. H. Wan and Z. N. Gu, *Mater. Sci. Eng., A*, 2000, **286**, 106.
26 J. F. Liu, K. Z. Yang and Z. H. Lu, *J. Am. Chem. Soc.*, 1997, **119**, 11 061.
27 E. Braun, Y. Eichen, U. Sivan and G. Ben Yoseph, *Nature*, 1998, **391**, 775.
28 T. J. Trentler, K. M. Hickman, S. C. Goel, A. M. Viano, P. C. Gibbons and W. E. Buhro, *Science*, 1995, **270**, 1791.
29 Z. A. Peng and X. G. Peng, *J. Am. Chem. Soc.*, 2001, **123**, 183.
30 Y. D. Li, H. W. Liao, Y. Ding, Y. T. Qian, L. Yang and G. E. Zhou, *Chem. Mater.*, 1998, **10**, 2301.
31 Y. D. Li, H. W. Liao, Y. Ding, Y. Fan, Y. Zhang and Y. T. Qian, *Inorg. Chem.*, 1999, **38**, 1382.
32 J. Yang, J. H. Zeng, S. H. Yu, L. Yang, G. E. Zhou and Y. T. Qian, *Chem. Mater.*, 2000, **12**, 3259.
33 Z. P. Qiao, Y. Xie, X. J. Li, C. Wang, Y. J. Zhu and Y. T. Qian, *J. Mater. Chem.*, 1999, **9**, 735.
34 J. H. Zhan, X. G. Yang, D. W. Wang, S. D. Li, Y. Xie, Y. Xia and Y. T. Qian, *Adv. Mater.*, 2000, **12**, 1348.
35 R. Sato, *Nature*, 1959, **184**, 2005.
36 L. A. Patil, P. A. Wani and D. P. Amalnerkar, *Mater. Chem. Phys.*, 1999, **61**, 260.
37 O. Zelaya-Angel and R. Lozada-Morales, *Phys. Rev. B*, 2000, **62**, 13 064.
38 A. Mews, A. V. Kadavanich, U. Banin and A. P. Alivisatos, *Phys. Rev. B: Condens. Matter*, 1996, **53**, 13 242.